Real-time Sub-THz link enabled purely by optoelectronics: 90-310 GHz seamless operation

Efstathios Andrianopoulos, Nikolaos K. Lyras, Evangelos Pikasis, Garrit Schwanke, Milan Deumer, Simon Nellen, Tianwen Qian, Georgia D. Ntouni, Eleftherios C. Loghis, Elias D. Tsirbas, Panteleimon-Konstantinos Chartsias, David de Felipe, Panos Groumas, Maria Massaouti, Christos Tsokos, Christos Kouloumentas, Dimitrios Kritharidis, Robert B. Kohlhaas, Norbert Keil, Martin Schell, and Hercules Avramopoulos.

***Abstract*—Optoelectronic technology is expected to be the cornerstone of sub-THz communication systems, enabling access to and use of the vast frequency resources found in this portion of the spectrum. In this work we demonstrate a photonics-enabled sub-THz wireless link operating in real-time settings, using a PIN-PD-based THz emitter, and a THz receiver based on an ultra-fast photoconductor. The real-time generation and detection of the information signal is performed by an intermediate frequency (IF) unit based on a commercially available mmWave platform, operating at 1.6 GBaud. The evaluation of our setup takes place on two phases. Firstly, a homodyne scenario is demonstrated, where the same pair of lasers is used at the transmitter and receiver side. Secondly, we demonstrate a heterodyne scheme, employing optical phase locking techniques at the receiver. Error-free operation was achieved in both scenarios at a bit rate of 3.2 Gb/s, over 1 m of free-space with ambient air. The broadband characteristics of our setup were validated, achieving error-free transmission over a 0.22 THz range, spanning from 90 up to 310 GHz. Finally, the stability of our real-time link was successfully demonstrated, showing stable SNR performance at the receiver with adaptive capabilities, over a time period of 5 min and 22 sec.**

***Index Terms*—Microwave photonics, sub-THz communications, phase locking, optical frequency comb, real-time communications, THz heterodyne detection, photoconductive antennas**

I. Introduction

Sub-Terahertz (0.1 – 0.3 THz) communications have been gaining significant interest in wireless communications systems, promising to fulfill the soaring demands for higher data rates towards the 6G communication era. The available spectral resources in this regime are considered as a key enabler of high-capacity short-distance applications of future wireless communication systems such as wireless personal area networks and wireless local area networks [1][2].

To that end, multiple approaches have been proposed aiming to develop solutions for the generation and detection of THz wave signals, including purely electronics-based solutions, as well as hybrid techniques employing optoelectronic technologies. Even though electronics-based technology is more mature than its photonic counterpart, their inherent bandwidth limitations render only a small part of the available spectral resources exploitable. Within this context, optoelectronics-based technology emerges as a promising solution, providing the ability to cover a large part of THz electromagnetic spectrum, whilst also providing seamless integration with high-speed fiber networks, enabling fiber-like communication over the air [3].

Optoelectronics based THz systems take advantage of emitters and receivers based on photoconductive antennas (PCAs), which have wide deployment in spectroscopy applications [4]-[6]. Whereas photodiodes are suited to drive emitting antennas, ultra-fast photoconductors serve for down-conversion at the receiving antennas. Additional requirements are needed however, for optoelectronic emitters and receivers to be used for heterodyne operation with broadband signals in THz communications, e.g., sufficient IF bandwidth, frequency stability and signal integrity [7]-[9].

For the realization of wireless sub-THz communication links employing optoelectronics, several experiments have already been conducted [10]-[15]. Significant efforts on this topic include the realization of hybrid links, using a combination of photonics-enabled emitters and electronic receivers, employing RF down-conversion methods consisted of cascaded RF local oscillators or sub-harmonic mixing processes, showcasing transmission of 24 Gb/s [10] and 160 Gb/s [11] data rates, over a central frequency of 300 GHz at a distance of 0.5 m. Purely optoelectronics THz links have been demonstrated utilizing PCAs as photonic receivers. Authors in [12] demonstrated a wireless link of 10 Gb/s data rate at 58 m distance, by utilizing a UTC-PD based transmitter and a THz-wave amplifier which however limited the link's exploitable frequency range from 0.24 to 0.34 THz. Additionally, the signal generation and demodulation were performed by high-tech test & measurement equipment such as arbitrary waveform generators and oscilloscopes, employing highly sophisticated DSP algorithms.

Under that context, optical phase locking techniques have been widely considered to compensate for the phase noise accommodated in optical heterodyne systems, enabling the generation of high-purity sub-THz carriers, alleviating the DSP

Manuscript received (Month) (day), 2022; revised (Month) (day), 2022; accepted (Month) (day), 2022. Date of publication (Month) (day), 2021; date of current version (Month) (day), 2022. This work was supported by the European Horizon 2020 Project ICT-TERAWAY.

E. Andrianopoulos, N. K. Lyras, C. Tsokos, M. Massaouti P. Groumas, Ch. Kouloumentas and H. Avramopoulos are with the Photonic Communications Research Laboratory at the National Technical University of Athens, Zografou 15573, Athens, Greece (efand@mail.ntua.gr).

P. Groumas and Ch. Kouloumentas are also with Optagon Photonics, Agia Paraskevi 15341, Athens, Greece (christos.kouloumentas@optagon-photonics.eu). G. Schwanke, M. Deumer, S. Nellen, T. Qian, D. Felipe, R. B. Kohlhaas, N. Keil and M. Schell are with the Fraunhofer Institute for Telecommunications, Heinrich-Hertz-Institut, Berlin 10587, Germany (simon.nellen@hhi.fraunhofer.de).

E. Pikasis, G. D. Ntouni, E. Loghis, E. C. Tsirbas, P.-K. Chartsias and D. Kritharidis are with Intracom Telecom 19.7 km Markopoulou Ave., Peania, 19002, Athens, Greece (epikasis@intracom-telecom.com).

requirements. Works under that topic include the transmission of a 400 GHz signal with a bit-rate of 106 Gb/s over 0.5 m [13], as well as a 50 Gb/s transmission at a distance of 100 m over a 300 GHz carrier [14] both enabled by hybrid photonic-electronic links. All-photonic based sub-THz link has been also demonstrated in [15] supporting 400 Mb/s capacity at 120 GHz carrier frequency at a distance of 0.25 m. These demonstrations however were based on either offline processing, or in real-time employing VSA software analysis. Exploitation and integration of sub-THz communication links in real communication systems in the 6G era would require data generating and processing tasks to be performed by digital circuit modules employing real-time solutions based on FPGAs or ASICs.

In this work we experimentally demonstrate a real-time wireless link operating in the sub-THz regime employing purely photonic components, transmitting QPSK signals at a fixed symbol rate of 1.6 GBaud. The real-time generation and detection of the RF signal is performed by an IF unit hosting a baseband modem based on a commercially available mmWave platform designed for E-band operation. This all-photonic network for the emission and detection of the wireless signal is enabled by an emitter based on a PIN-PD [4][8] and a receiver based on an ultra-fast photoconductor [16] both with integrated broadband antennas, mounted on a silicon lens for radiation into free-space, and packaged into a fiber-pigtailed housing. The demonstration presented in this paper is two-fold. Firstly, our link was evaluated in a homodyne scenario where the same pair of lasers is used in the transmitter and receiver part for the generation and detection of the sub-THz signals. Secondly, in a more realistic scenario, a heterodyne detection scheme was implemented, where the optical sources are uncorrelated and phase noise phenomena become more dominant. Phase locking techniques were implemented in this case, by injecting an optical frequency comb into a set of tunable lasers. To the best of our knowledge, this is the first demonstration of a real-time wireless link, based on an all-photonic architecture.

II. Homodyne Scenario: Setup & Results

Figure 1 depicts the experimental setup in the homodyne scenario. Two tunable laser sources are split equally towards the transmitter (Tx) and receiver (Rx) part. At the Tx side, the first tone (TL1) is modulated by means of a Mach-Zehnder modulator (MZM) by a QPSK signal of 1.6 GBaud symbol rate, at an intermediate frequency (IF) $f_{IF} = 5$ GHz generated from the IF unit. The I/Q signal components are generated by an FPGA-based baseband board through digital-to-analog converters (DACs), and are upconverted to the fixed IF via an IF board in the IF unit, hosting DA/AD converters and I/Q modulators/demodulators for the IF up/down-conversion. The developed DSP methods enable the encapsulation of Ethernet packets inside wireless transmission frames. An efficient concatenated forward error correction (FEC) scheme based on Low Density Parity Check and Reed Solomon encoding is employed, and dedicated DSP modules implement different procedures like filtering for sampling rate conversion and pulse shaping, equipped with DAC interfaces.

The output of the MZM is amplified by an erbium-doped fiber amplifier (EDFA), followed by an optical bandpass filter

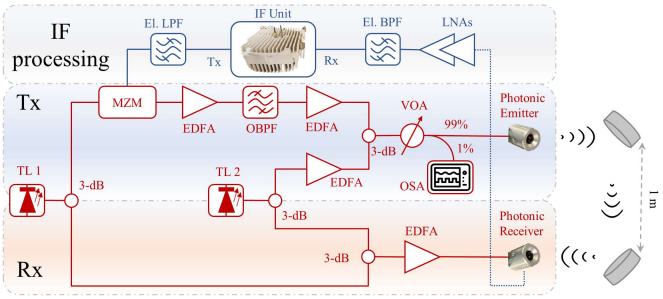

Figure 1: Homodyne case - Schematic of the experimental setup

(OBPF) suppressing one of the two sidebands and the carrier. The two paths comprising the Tx are then amplified by means of EDFAs and coupled together, before being fed into the photonic THz emitter. The emitter then down-converts the optical signal to the electrical domain and radiates the signal at a frequency equal to the difference of the frequencies of the two optical paths ($f_{THz} = |f_{TL1} - f_{TL2} + f_{IF}|$). Off-axis parabolic mirrors with 2-inch diameter and 3-inch focal length are placed both after the output of the Tx and before the input of the Rx to increase the antenna gain and guide the transmitted beam across 1 m of free-space with ambient air.

At the Rx part, the two tones generated by TL1 and TL2 are coupled together and amplified, serving as the optical input of the photonic THz receiver. The optoelectronic receiver module is similar to the heterodyne receiver reported in [16] but with improved electrical design for increased IF bandwidth and improved photoconductive material for better conversion efficiency [6]. The PCA uses the beat signal of the two tones and generates a photonic local oscillator (PLO) ($f_{PLO} = |f_{TL1} - f_{TL2}|$) to down-convert the received THz signal. In the homodyne detection scheme, the IF signal at the output of the Rx is equal to the offset frequency of the data modulation from the IF unit: $f_{IF} = |f_{THz} - f_{PLO}|$. After down-conversion, the IF signal is processed by an analog microwave chain comprising two low-noise amplifiers and a bandpass filter.

When the signal is received by the IF unit, the I/Q down-conversion process takes place and the produced distorted QAM signals are captured by the ADCs. Next, the FPGA recovers the I/Q data streams and performs all the appropriate DSP functions such as symbol timing, frame synchronization, carrier frequency offset cancelation, phase noise correction, filtering, equalization, RF impairments compensation, symbol de-mapping, and FEC decoding. Finally, the modem extracts real-time key performance indicators, such as the constellation diagram, signal to noise ratio (SNR) and bit error ratio (BER). The BER is not extracted through EVM estimations, but is rather measured comparing the generated and received PRBS traffic, providing real BER measurements. The SNR values are calculated from the extracted constellation diagram in real time.

In the first demonstration scenario we assessed the frequency response of our link, performing frequency-relative measurements by tuning the unmodulated laser tone (TL2), without modifying the setup. The photocurrent value of the emitter remained fixed at 12 mA during all measurements, corresponding to an optical input power of 15 dBm. Figure 2 depicts the BER and SNR values as a function of the central frequency of the emitted signal. Since the modules are originally designed for frequencies beyond 100 GHz, the lower cut-off frequency of the antenna structure leads to decreased

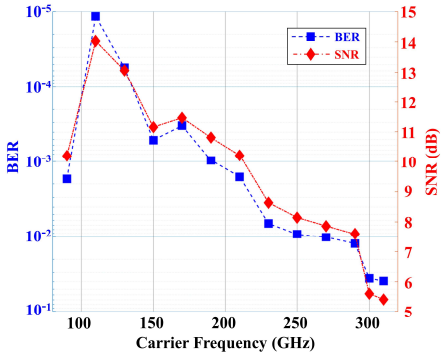

Figure 2: Homodyne case - BER & SNR with respect to the frequency of the generated sub-THz carrier.

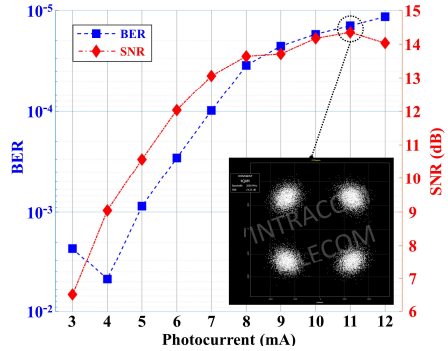

Figure 3: Homodyne case - BER & SNR with respect to the emitter's photocurrent. Inset: Real-time constellation diagram

performance below 100 GHz. As the frequency increases, the SNR of our link decreases, following a proportional relationship with the frequency response of the photonic transceiver modules. However, error-free performance in a frequency span of 220 GHz was achieved post-FEC encoding using the same setup, validating the ultra-broadband characteristics of our link in real time. The worst-case BER pre-FEC in all the cases examined (i.e., 90-310 GHz) was $3.9 \cdot 10^{-2}$.

Figure 3 presents the real-time BER and SNR values with respect to the DC photocurrent at the photonic emitter. Note that the photocurrent is proportional to the emitted THz power [11]. The central frequency of the signal was set at 110 GHz found to be the optimal frequency point in terms of link performance. As can be observed from the figure, the link exhibits good performance even for the lowest values of the photocurrent, achieving error-free performance post FEC encoding. A screenshot of the monitor interface of the IF unit is depicted as inset, showcasing the real-time constellation diagram of the received QPSK signal, corresponding to a DC photocurrent value of 11 mA. This interface allows us to assess the performance of our link in real-time, providing information on among others the SNR and BER values.

III. Heterodyne Scenario: Setup & Results

Having validated the successful operation of our link in a homodyne setup, heterodyne scenarios were assessed emulating a more realistic scenario. Starting off, an extra pair of tunable lasers were implemented at the Rx side of Figure 1, completely uncorrelated in terms of phase noise with the ones of the Tx side, as well as with each other. However, it was quickly identified that such a link could not have a stable real-time performance over a long period of time, due to the phase

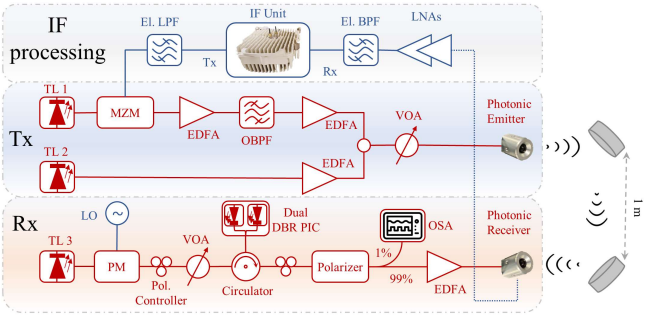

Figure 4: Heterodyne case - Schematic of the experimental setup

noise of essentially four uncorrelated laser sources. Therefore, phase-locking techniques to alleviate this issue.

More specifically, as depicted in Figure 4, in the heterodyne scenario the Tx path follows the same rationale as for the homodyne case. For the Rx part, a different tunable laser source (TL3) serves as the optical input of the optical frequency comb generation (OFCG) unit, which is implemented by means of a phase modulator (PM) driven by a sinusoidal wave generated by an RF local oscillator. At the output of the OFCG, an optical circulator is responsible for the injection of the optical frequency comb into a dual Polymer-InP DBR laser chip, implementing the phase locking process. This concept has been extensively described in [17]. The resulting phase-locked carriers are then amplified by an EDFA and forwarded to the photonic THz receiver to enable the down-conversion process. We note that even though the setup is based on polarization maintaining fibers, the output fiber of our PM and the pigtailed fiber of the dual DBR laser chips were SSMFs. Therefore, polarization handling equipment (i.e., 2 polarization controllers and a polarizer) was used to optimize the locking process, as well as the photomixing process at the photonic THz receiver.

Figure 5 presents the real-time BER and SNR values for the heterodyne scenario as a function of the DC photocurrent in the photonic THz emitter. The central frequency of the emitted signal remained fixed at 110 GHz. Compared to the homodyne respective results depicted in Figure 3, the heterodyne scenario expectedly exhibits a slightly worse performance. The reason behind this is derived from the nature of homodyne systems, where the beating terms of the two tones at the Tx and Rx side are correlated in terms of phase characteristics. Therefore, the frequency instability of the two beating terms cancels out, providing a stable signal in terms of frequency at the IF unit's input. This is not the case however in the heterodyne scenario where, even though the beating term of the two phase-locked tones at the Rx side exhibits excellent phase noise characteristics [17], the beating term at the Tx side results from two uncorrelated laser tones, inevitably transferring the frequency and phase instabilities to the RF domain. Nevertheless, error-free performance was also achieved in this case, with a worst-case pre-FEC BER of $4.12 \cdot 10^{-2}$.

To assess the real-time performance of our link, time-relative measurements of the received SNR were performed. Figure 6 depicts a 5 min and 22 sec snapshot of the SNR as a function of time. During these measurements, the photocurrent was 12 mA, and the central frequency of the signal remained the same. A zoomed-in version is presented as inset in the figure, showcasing the SNR deviation in this time frame. As can be seen from the figure, the employment of optical injection

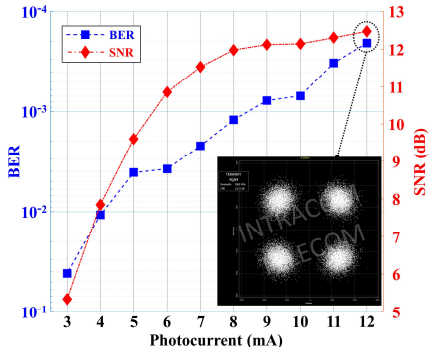

Figure 5: Heterodyne case - BER & SNR with respect to the emitter's photocurrent. Inset: Real-time constellation diagram

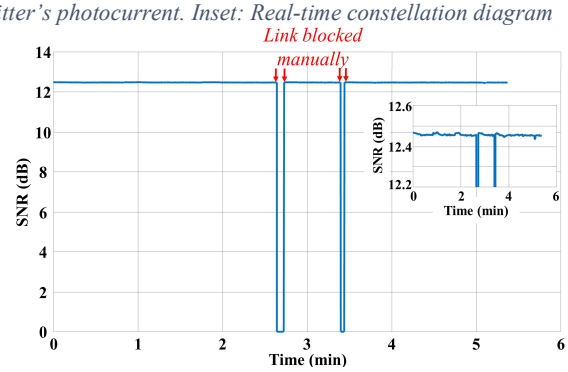

Figure 6: Heterodyne case – Time-relative SNR measurement. Red arrows depict the time frames where the link was manually blocked.

locking technique to compensate for the phase noise accumulated in an all-photonic scenario, enabled the very stable real-time performance of our photonics-enabled sub-THz link. Two SNR deeps can be observed shortly before and after the 3-minute point mark, where the link was manually blocked using a metallic plate. Even though during the blockage time the link was completely lost, the system's adaptive algorithms were able to re-initiate and stabilize the link automatically to the exact same point, when the blockage was removed.

IV. Conclusions

We have demonstrated for the first time a real time sub-THz wireless link, enabled purely by optoelectronic technology. The real time aspect of our demonstration was based on an IF unit generating and detecting QPSK signals at 1.6 GBaud. Wireless transmission over 1 m was performed, enabled by a PIN-PD based emitter and a PCA based receiver paired with off-axis parabolic mirrors. Our setup was evaluated in a two-fold approach, employing a homodyne scenario where the same pair of lasers were used in both Tx and Rx side, and a heterodyne scenario enabled by optical phase locking techniques at the Rx. Error-free operation was achieved in both scenarios, for all values of the generated photocurrent at the photonic emitter. Moreover, the ultra-broadband characteristics of our link were validated in real time, achieving real time error-free operation in a frequency span of 220 GHz (90-310 GHz). The link's stability over time was showcased in the heterodyne scenario, showcasing stable performance with adaptive characteristics. This work sets a basis towards concrete exploitation of the sub-THz band, which could be implemented by miniaturizing the transceivers into compact optical engines, leveraging the advancements of photonic integration technologies [18].

Acknowledgments

This work was supported by TERAWAY project, funded from European Union's Horizon 2020 R&I Programme under G.A No 871668, initiative of Photonics PPP.

References

[1] Song, H.-J., and Nagatsuma, T.: 'Present and future of terahertz communications', Trans. THz Sci. Technol, 2011, 1, (1), pp. 256–263.
[2] S. Rommel et al., "Data center connectivity by 6G wireless systems," in Proc. Photon. Switching Comput., Sep. 2018
[3] J. Zhang et al., "Real-time Demonstration of 100 GbE THz-wireless and Fiber Seamless Integration Networks," in JLT, 2022.
[4] S. Preu et al., "Tunable, continuous-wave terahertz photomixer sources and applications," J. Appl. Phys. 109(6), 061301-1-061301–56 (2011).
[5] S. Nellen, et.al., "Experimental Comparison of UTC- and PIN-Photodiodes for Continuous-Wave Terahertz Generation," JIMTW 41(4), 343–454 (2020).
[6] M. Deumer, et.al., "Continuous wave terahertz receivers with 4.5 THz bandwidth and 112 dB dynamic range," Opt. Express 29(25), 41819 (2021).
[7] Y. J. Lin and M. Jarrahi, "Heterodyne terahertz detection through electronic and optoelectronic mixers," Reports Prog. Phys. 83(6), (2020).
[8] S. Nellen, et.al., "Radiation pattern of planar optoelectronic antennas for broadband continuous-wave terahertz emission," Opt. Express 29(6), 8244 (2021).
[9] G. Carpintero, et.al., "Wireless Data Transmission at Terahertz Carrier Waves Generated from a Hybrid InP-Polymer Dual Tunable DBR Laser Photonic Integrated Circuit," Sci. Rep. 8(1), 1–7 (2018).
[10] Song, H.-J et al., "24 Gbit/s data transmission in 300 GHz band for future terahertz communications" Electronics Letters, 2012, 48, (15), p. 953-954.
[11] S. Nellen et al., "Coherent Wireless Link at 300 GHz With 160 Gbit/s Enabled by a Photonic Transmitter," in JLT, vol. 40, no. 13, pp. 4178-4185, 1 July1, 2022.
[12] Tobias Harter et al.,"Wireless THz link with optoelectronic transmitter and receiver," Optica 6, 1063-1070(2019)
[13] S. Jia et al., "0.4 THz Photonic-Wireless Link With 106 Gb/s Single Channel Bitrate," in Journal of Lightwave Technology, vol. 36, no. 2, pp. 610-616, 15 Jan.15, 2018.
[14] T. Nagatsuma et al., "300-GHz-band wireless transmission at 50 Gbit/s over 100 meters," 2016 41st IRMMW-THz, 2016, pp. 1-2.
[15] A. Morales et al., "Highly Tunable Heterodyne Sub-THz Wireless Link Entirely Based on Optoelectronics," in IEEE Transactions on Terahertz Science and Technology, vol. 11, no.3, pp. 261-268, 2021.
[16] S. Nellen et al., "Fiber-coupled, photoconductive receiver for heterodyne detection up to 1 THz stabilized by an optical frequency comb," 2017 42nd IRMMW-THz.
[17] E. Andrianopoulos et al., "Optical Generation and Transmission of mmWave Signals in 5G ERA: Experimental Evaluation Paradigm," in IEEE PTL vol. 34, no. 19, pp. 1011-1014, 1 Oct.1, 2022.
[18] https://ict-teraway.eu/